

INHOMOGENEOUS BEAM OF LINEARLY VARYING HEIGHT UNDER THREE-POINT BENDING: A LONGITUDINAL FRACTURE ANALYSIS

NEHOMOGENI NOSAČ LINEARNO PROMENLJIVE VISINE OPTEREĆEN SAVIJANJEM U TRI TAČKE: PODUŽNA ANALIZA LOMA

Originalni naučni rad / Original scientific paper
UDK /UDC:

Rad primljen / Paper received: 14.01.2020

Adresa autora / Author's address:
University of Architecture, Civil Engineering and Geodesy,
Department of Technical Mechanics, Sofia, Bulgaria,
email: v_rizov_fhe@uacg.bg

Keywords

- inhomogeneous beam
- longitudinal fracture
- material nonlinearity
- bending

Abstract

The paper deals with longitudinal fracture analysis of an inhomogeneous beam of linearly varying height of cross-section along the beam length. The beam is under three-point bending. The beam height increases linearly from the two ends towards the mid-span. A longitudinal crack is located arbitrary along the beam height. The beam exhibits continuous (smooth) material inhomogeneity along its height and length. The material is nonlinear elastic. Longitudinal fracture behaviour of the beam is studied in terms of strain energy release rate. Energy balance is analysed in order to derive a solution to the strain energy release rate. The solution is verified by applying the J-integral approach. The solution is used to investigate influences of linearly varying beam height in length direction; material inhomogeneity along the beam height and length; location of crack along beam height and crack length on longitudinal fracture behaviour. Longitudinal fracture analysis developed here can be used in the preliminary design of load-bearing inhomogeneous nonlinear elastic beam structures with continuously varying height in the length direction.

INTRODUCTION

The usage of beams of varying height of the cross-section along beam length is wide-spread in various advanced load-bearing structures in modern civil and mechanical engineering. This is due mainly to the fact that the beams of varying height can provide a very efficient distribution of strength and stiffness in engineering structures. Thus, the beams of varying height are very suitable for increasing the strength and stiffness and for improving the stability of structures. At the same time, by using beams of varying height, one can significantly reduce the weight of structures.

Beam structures of varying height can be manufactured by inhomogeneous materials. The most important feature of inhomogeneous materials is the continuous variation of their properties along one or more spatial coordinates in the volume of the structural member. Therefore, the material properties of inhomogeneous materials are continuous (smooth) functions of coordinates. Typical kind of inhomogeneous structural materials are functionally graded materials which have been used extensively in aeronautics, nuclear reactors, chemical engineering, electronics, mechanical engineering and biomedicine /1-4/. Functionally graded materials are new inhomogeneous composites manufactured by mixing two or more constituent materials. Graded distribution of the material properties of functionally graded materials is formed technologically so as to satisfy the requirements for different parts of a structural member. Fracture behaviour of inhomogeneous materials is of great importance for structural integrity of inhomogeneous load-bearing structures. Therefore, considerable attention has been paid by the research community to analyse the fracture behaviour of inhomogeneous (functionally graded) materials and structures, /5-7/.

Ključne reči

- nehomogeni nosač
- podužni lom
- nelinearan materijal
- savijanje

Izvod

U radu je obrađena analiza podužnog loma nehomogenog nosača, linearno promenljive visine poprečnog preseka po dužini nosača. Nosač je opterećen savijanjem u tri tačke. Visina nosača se povećava linearno, od njegovih krajeva ka sredini. Podužna prslina je locirana proizvoljno po visini nosača. Nosač ispoljava kontinualno (glatko) nehomogeno ponašanje materijala po visini i dužini. Materijal se ponaša nelinearno elastično. Podužni lom nosača je razmotren preko brzine oslobađanja deformacione energije. Analizom balansa energije je dobijeno rešenje za brzinu oslobađanja deformacione energije. Rešenje je provereno primenom koncepta J integrala. Rešenje se koristi za istraživanje uticaja linearne promene visine nosača u pravcu dužine; nehomogenost materijala po visini i dužini nosača; položaju prsline po visini nosača i dužini prsline na ponašanje podužnog loma. Analiza podužnog loma predstavljena u radu se može primeniti u preproračunu konstrukcija sa opterećenim nehomogenim nelinearno elastičnim nosačima, kod kojih se kontinualno menja visina u pravcu dužine.

geneous structural materials are functionally graded materials which have been used extensively in aeronautics, nuclear reactors, chemical engineering, electronics, mechanical engineering and biomedicine /1-4/. Functionally graded materials are new inhomogeneous composites manufactured by mixing two or more constituent materials. Graded distribution of the material properties of functionally graded materials is formed technologically so as to satisfy the requirements for different parts of a structural member. Fracture behaviour of inhomogeneous materials is of great importance for structural integrity of inhomogeneous load-bearing structures. Therefore, considerable attention has been paid by the research community to analyse the fracture behaviour of inhomogeneous (functionally graded) materials and structures, /5-7/.

Various problems of fracture mechanics of functionally graded materials have been analysed in /5/. Methods for solving crack problems in functionally graded materials are

developed by applying linear-elastic fracture mechanics, i.e. the assumption for linear-elastic behaviour has been used. Solutions of some benchmark problems have been derived and discussed in detail. It has been shown that the results obtained can provide technical support for design engineers and material scientists working in the field of graded materials.

Various publications in the area of fracture behaviour of functionally graded composite materials have been considered in /6/. Both static and fatigue crack problems have been discussed. Solutions of different crack problems obtained assuming linear-elastic mechanical behaviour of the graded material have been presented. Investigations of fracture behaviour under thermal loading and under contact loading have been carried out. Different mathematical descriptions of the material gradient have been considered and analysed.

Analyses of cracks in functionally graded materials have been performed in /7/. Methods of linear-elastic fracture mechanics have been applied. Fracture behaviour has been studied as a function of crack length. Comparisons between results obtained by using linear law for variation of the modulus of elasticity and results derived assuming discrete approximation in a multi-layered beam configuration have been carried out.

The above publications are focused on fracture analyses of inhomogeneous (functionally graded) materials which are carried out assuming linear elastic behaviour. Recently, works on longitudinal fracture of functionally graded beam structures which exhibit nonlinear mechanical behaviour of the material have also been published /8-10/. These works, however, are concerned with beams of constant cross-section along the beam length, /8-10/.

Therefore, the purpose of the present paper is to develop a longitudinal fracture analysis of an inhomogeneous beam of linearly varying height. The beam is loaded in three-point bending. The material of the beam has nonlinear elastic behaviour. Fracture is studied in terms of strain energy release rate by considering the balance of energy. The J-integral approach is applied for verification.

LONGITUDINAL FRACTURE ANALYSIS

The simply supported inhomogeneous beam shown in Fig. 1 is loaded by one vertical force, F , applied in the mid-span, i.e. the beam is subjected to three-point bending. The length of the beam is denoted by $2l$.

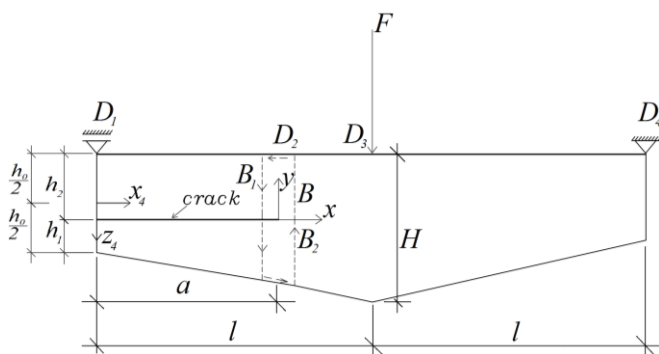


Figure 1. Geometry and loading of an inhomogeneous beam configuration of linearly varying height along beam length.

The beam exhibits continuous (smooth) material inhomogeneity in both height and length directions. Besides, the material has nonlinear elastic mechanical behaviour. The cross-section of the beam is a rectangle of width b , and height h . The height varies linearly from h_0 in the two ends of the beam to H in the mid-span (Fig. 1). Thus, the variation of h in beam portion, D_1D_3 , is written as

$$h = h_0 + \frac{H - h_0}{l} x_4, \tag{1}$$

where

$$0 \leq x_4 \leq l. \tag{2}$$

The longitudinal axis, x_4 , is shown in Fig. 1. In the beam portion, D_3D_4 , the variation of h is expressed as (Fig. 1)

$$h = H - \frac{H - h_0}{l} (x_4 - l), \tag{3}$$

where

$$l \leq x_4 \leq 2l. \tag{4}$$

Thus, the beam geometry is symmetrical with respect to the mid-span.

A longitudinal crack of length a , is located in the beam as shown in Fig. 1 (it should be mentioned that the present fracture study is motivated also by the fact that certain kinds of inhomogeneous materials, such as functionally graded materials, can be built-up layer-by-layer /11/ which is a premise for the appearance of a longitudinal crack between layers). The heights of the lower and upper crack arms in the left-hand end of the beam are denoted by h_1 and h_2 , respectively. Besides, the height of the lower crack arm h_{1r} , increases linearly along the crack length

$$h_{1r} = h_1 + \frac{H - h_0}{l} x_4, \tag{5}$$

where

$$0 \leq x_4 \leq a. \tag{6}$$

The height of the upper crack arm is constant (Fig. 1). Apparently, the lower crack arm is free of stresses (Fig. 1).

The mechanical behaviour of the material is treated by applying the following nonlinear stress-strain relation /12/:

$$\sigma = S \left[1 - \left(1 - \frac{\varepsilon}{R} \right)^m \right], \tag{7}$$

where: S , R and m are material properties. The distribution of S along the height of the beam cross-section is described by the following power law:

$$S = S_g + \frac{S_d - S_g}{h^n} \left(\frac{h}{2} + z_5 \right)^n, \tag{8}$$

where

$$-\frac{h}{2} \leq z_5 \leq \frac{h}{2}. \tag{9}$$

In Eq.(8), S_g and S_d are the values of S in the upper and lower surface of the beam, respectively; n is a material property that controls the material inhomogeneity along the beam height; z_5 is the vertical centroidal axis of the beam cross-section. Material properties, S_g and S_d , vary in the length direction in beam portion D_1D_3 , according to the following power laws:

$$S_g = S_{gh} + \frac{S_{gH} - S_{gh}}{l^r} x_4^r, \quad (10)$$

$$S_d = S_{dh} + \frac{S_{dH} - S_{dh}}{l^f} x_4^f, \quad (11)$$

where

$$0 \leq x_4 \leq l. \quad (12)$$

In Eq.(10), S_{gh} and S_{gH} are the values of S_g in the left-hand end of the beam and the mid-span, respectively; r is a material property that controls the material inhomogeneity in the length direction at the upper surface of the beam. In Eq.(11), S_{dh} and S_{dH} are the values of S_d in the left-hand end of the beam and mid-span, respectively; material property f , controls the material gradient along the length of the beam at the lower surface of the beam. The variation of S_g and S_d in the beam portion D_3D_4 , is written as

$$S_g = S_{gH} - \frac{S_{gH} - S_{gh}}{l^r} (x_4 - l)^r, \quad (13)$$

$$S_d = S_{dH} - \frac{S_{dH} - S_{dh}}{l^f} (x_4 - l)^f, \quad (14)$$

where

$$l \leq x_4 \leq 2l. \quad (15)$$

The longitudinal fracture behaviour is studied in terms of strain energy release rate, G . The balance of energy is considered in order to derive the strain energy release rate. For this purpose, assuming a small increase δa , of the crack length, the energy balance is expressed as

$$F \delta w = \frac{\partial U}{\partial a} \delta a + G b \delta a, \quad (16)$$

where: U is strain energy in the beam; δw is the increase in vertical displacement of the external force application point F . From Eq.(16), the strain energy release rate is derived as

$$G = \frac{F}{b} \frac{\partial w}{\partial a} - \frac{1}{b} \frac{\partial U}{\partial a}. \quad (17)$$

Vertical displacement of force application point, F , is obtained by applying Maxwell-Mohr integrals. The result is (Fig. 1),

$$w = \int_0^a \frac{1}{2} x_4 \kappa_1 dx_4 + \int_a^l \frac{1}{2} x_4 \kappa_2 dx_4 + \int_l^{2l} \left(l - \frac{x_4}{2} \right) \kappa_3 dx_4, \quad (18)$$

where: κ_1 , κ_2 and κ_3 are curvatures of upper crack arm and beam portions D_2D_3 and D_3D_4 , respectively.

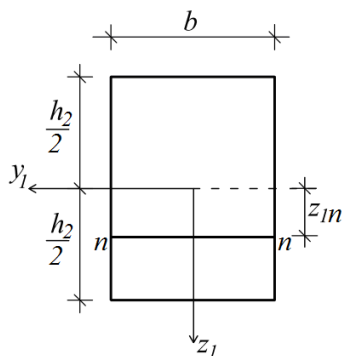


Figure 2. Cross-section of upper crack arm (n - n is the position of neutral axis).

Curvature of the upper crack arm is obtained by using the equations for equilibrium of elementary forces in the cross-section of the upper crack arm,

$$N_1 = b \int_{-\frac{h_2}{2}}^{\frac{h_2}{2}} \sigma dz_1, \quad (19)$$

and

$$M_{y_1} = b \int_{-\frac{h_2}{2}}^{\frac{h_2}{2}} \sigma z_1 dz_1, \quad (20)$$

where: N_1 and M_{y_1} are the axial force and bending moment in the cross-section; σ is the normal stress; z_1 is the vertical centroidal axis of cross-section (Fig. 2). It is obvious that (Fig. 1),

$$N_1 = 0, \quad (21)$$

$$M_{y_1} = \frac{F}{2} x_4, \quad (22)$$

where

$$0 \leq x_4 \leq l. \quad (23)$$

The normal stress involved in Eqs.(19) and (20) is expressed as a function of strain by Eq.(7). The distribution of strains along the height of the upper crack arm is treated by applying Bernoulli's hypothesis for plane sections, since a beam of a high length-to-height ratio is under consideration here. Thus, ε is written as

$$\varepsilon = \kappa_1 (z_1 - z_{1n}), \quad (24)$$

where

$$-\frac{h_2}{2} \leq z_1 \leq \frac{h_2}{2}. \quad (25)$$

In Eq.(24), κ_1 and z_{1n} are the curvature and coordinate of the neutral axis. It should be mentioned that the neutral axis shifts from the centroid since the beam exhibits material inhomogeneity in the height direction (Fig. 2). By using Eq.(8), the variation of S along the height of the upper crack arm is expressed as

$$S = S_g + \frac{S_d - S_g}{h^n} \left(z_1 + \frac{h_2}{2} \right)^n, \quad (26)$$

where: z_1 changes within interval Eq.(25). After substituting Eqs.(7), (21), (22), (24) and (26) in Eqs.(19) and (20), the two equations for equilibrium are solved with respect to κ_1 and z_{1n} by applying the MatLab® computer program.

The curvature of the beam in portion D_2D_3 , is obtained by using Eqs.(19) and (20). For this purpose, σ , h_2 and z_1 are replaced with $\sigma_{D_2D_3}$, h and z_2 , respectively. The normal stress $\sigma_{D_2D_3}$, in the cross-section of the beam in portion D_2D_3 , is obtained by replacing ε with $\varepsilon_{D_2D_3}$ in Eq.(7). The distribution of strains $\varepsilon_{D_2D_3}$, along the height of the beam in portion D_2D_3 , is found by replacing κ_1 , z_{1n} and z_1 with κ_2 , z_{2n} and z_2 in Eq.(24).

In order to determine the beam curvature in portion D_3D_4 , the quantities, σ , h_2 and z_1 are replaced, respectively, with $\sigma_{D_3D_4}$, h and z_3 in Eqs.(19) and (20). The strain, ε , is

replaced with $\varepsilon_{D_3D_4}$ in Eq.(7) to obtain the normal stress $\sigma_{D_3D_4}$, in the cross-section of beam portion D_3D_4 . Equation (24) is used to express distribution of strain $\varepsilon_{D_3D_4}$, along the height of beam portion D_3D_4 . For this purpose, κ_1, z_{1n} and z_1 are replaced with κ_3, z_{3n} and z_3 , respectively.

Since the lower crack arm is free of stresses, the strain energy stored in the beam is written as (Fig. 1)

$$U = U_1 + U_2 + U_3, \tag{27}$$

where: U_1, U_2 and U_3 are strain energies in the upper crack arm in portions D_2D_3 and D_3D_4 , of the beam, respectively.

The strain energy in the upper crack arm is expressed as

$$U_1 = \int_0^{\frac{b}{2}} \int_{-\frac{b}{2}}^{\frac{h_2}{2}} \int_0^{\frac{h_2}{2}} u_{01} dx_4 dy_1 dz_1, \tag{28}$$

where: u_{01} is the strain energy density, determined by using the following formula:

$$u_{01} = \int_0^{\varepsilon} \sigma(\varepsilon) d\varepsilon. \tag{29}$$

By substituting Eq.(7) in Eq.(29), one obtains

$$u_{01} = S\varepsilon + \frac{SR}{m+1} \left(1 - \frac{\varepsilon}{R}\right)^{m+1} - \frac{SR}{m+1}. \tag{30}$$

The strain energy in portion D_2D_3 of the beam is written as

$$U_2 = \int_a^l \int_{-\frac{b}{2}}^{\frac{h}{2}} \int_{-\frac{b}{2}}^{\frac{h}{2}} u_{02} dx_4 dy_2 dz_2, \tag{31}$$

where the strain energy density u_{02} , is obtained by applying Eq.(30). For this purpose, ε is replaced with $\varepsilon_{D_2D_3}$.

In beam portion D_3D_4 , the strain energy is found as

$$U_3 = \int_l^{\frac{2l}{2}} \int_{-\frac{b}{2}}^{\frac{h}{2}} \int_{-\frac{b}{2}}^{\frac{h}{2}} u_{03} dx_4 dy_3 dz_3, \tag{32}$$

where: u_{03} is the strain energy density. Equation (30) is used to calculate u_{03} by replacing ε with $\varepsilon_{D_3D_4}$.

Finally, by substituting Eqs.(18), (27), (28), (31) and Eq.(32) in Eq.(17), one derives the following expression for the strain energy release rate:

$$G = \frac{F}{b} \left(\frac{1}{2} a \kappa_1 - \frac{1}{2} a \kappa_2 \right) - \frac{1}{b} \left(\int_{-\frac{b}{2}}^{\frac{b}{2}} \int_{-\frac{b}{2}}^{\frac{h_2}{2}} u_{01} dy_1 dz_1 - \int_{-\frac{b}{2}}^{\frac{b}{2}} \int_{-\frac{b}{2}}^{\frac{h}{2}} u_{02} dy_2 dz_2 \right) \tag{33}$$

Integration in Eq.(33) is performed by using the MatLab computer program. It should be mentioned that $h, \kappa_1, \kappa_2, u_{01}$ and u_{03} involved in Eq.(33) are obtained by Eqs.(1), (19), (20) and Eq.(30) at $x_4 = a$.

In order to verify the solution of the strain energy release rate Eq.(33), the longitudinal fracture behaviour of the beam is analysed also by applying the J-integral approach, [13]. The J-integral is solved along the contour of integration, B , shown by a dashed line in Fig. 1. Since the lower crack arm is free of stresses, the solution of the J-integral is written as

$$J = J_{B_1} + J_{B_2}, \tag{34}$$

where: J_{B_1} and J_{B_2} are the J-integral values in segments B_1 and B_2 of the integration contour, respectively. It should be noted that segments B_1 and B_2 , coincide with cross-sections of the upper crack arm and the beam portion D_2D_3 , respectively.

In segment B_1 of the integration contour, the J-integral is expressed as

$$J_{B_1} = \int_{B_1} \left[u_{01} \cos \alpha_{B_1} - \left(p_{x_{B_1}} \frac{\partial u}{\partial x_{B_1}} + p_{y_{B_1}} \frac{\partial v}{\partial x_{B_1}} \right) \right] ds_{B_1}, \tag{35}$$

where the angle between the outwards normal vector to the contour of integration and the crack direction is marked by α_{B_1} ; the components of the stress vector are marked by $p_{x_{B_1}}$ and $p_{y_{B_1}}$; the components of the displacement vector with respect to the coordinate system, xy , are marked by u and v ; and ds_{B_1} is a differential element along the contour of integration.

The components of J_{B_1} are obtained as (Fig. 1)

$$p_{x_{B_1}} = -\sigma, \tag{36}$$

$$p_{y_{B_1}} = 0, \tag{37}$$

$$ds_{B_1} = dz_1, \tag{38}$$

$$\frac{\partial u}{\partial x_{B_1}} = \varepsilon, \tag{39}$$

$$\cos \alpha_{B_1} = -1. \tag{40}$$

Equations (7) and (24) are used to determine σ and ε , in respect. The strain energy density u_{01} , involved in Eq.(35) is found by Eq.(30). The coordinate z_1 , changes in the interval $[-h_2/2; h_2/2]$. By substituting Eqs.(36)-(40) in Eq.(35), one obtains

$$J_{B_1} = \int_{-\frac{h_2}{2}}^{\frac{h_2}{2}} (-u_{01} + \sigma \varepsilon) dz_1. \tag{41}$$

The J-integral in segment B_2 , of the integration contour is written as (Fig. 1)

$$J_{B_2} = \int_{B_2} \left[u_{02} \cos \alpha_{B_2} - \left(p_{x_{B_2}} \frac{\partial u}{\partial x_{B_2}} + p_{y_{B_2}} \frac{\partial v}{\partial x_{B_2}} \right) \right] ds_{B_2}, \tag{42}$$

where

$$p_{x_{B_2}} = \sigma_{D_2D_3}, \tag{43}$$

$$p_{y_{B_2}} = 0, \tag{44}$$

$$ds_{B_2} = -dz_2, \tag{45}$$

$$\frac{\partial u}{\partial x_{B_2}} = \varepsilon_{D_2D_3}, \tag{46}$$

$$\cos \alpha_{B_2} = 1. \tag{47}$$

By substituting Eqs.(43)-(47) into Eq.(42), one derives

$$J_{B_2} = \int_{-\frac{h}{2}}^{\frac{h}{2}} (u_{02} - \sigma_{D_2D_3} \varepsilon_{D_2D_3}) dz_2. \tag{48}$$

By substituting Eq.(41) and Eq.(48) into Eq.(34), one obtains the following expression for the J-integral:

$$J = \int_{-\frac{h_2}{2}}^{\frac{h_2}{2}} (-u_{01} + \sigma \varepsilon) dz_1 + \int_{-\frac{h}{2}}^{\frac{h}{2}} (u_{02} - \sigma_{D_2 D_3} \varepsilon_{D_2 D_3}) dz_2, \quad (49)$$

where: h , σ , $\sigma_{D_2 D_3}$, ε , $\varepsilon_{D_2 D_3}$, u_{01} and u_{03} are obtained by Eqs.(1), (7), (24) and Eq.(30) at $x_4 = a$. The integration in Eq.(49) is carried out by using MatLab®. The J-integral value obtained by Eq.(49) matches exactly the strain energy release rate found by Eq.(33). This fact is a verification of the longitudinal fracture analysis performed here.

NUMERICAL RESULTS

The solution to the strain energy release rate, Eq.(33), is used to investigate the influences of linearly varying height of the cross-section along the beam length, the continuous material inhomogeneity in the length and height directions, the crack location along the beam height and the crack length on the longitudinal fracture behaviour of the beam (Fig. 1). The strain energy release rate is presented in non-dimensional form by using the formula $G_N = G/(S_{gh}b)$. It is assumed that: $l = 0.080$ m; $h_0 = 0.004$ m, $b = 0.008$ m and $F = 4$ N. The variation of beam height in the length direction is characterized by h/h_0 ratio. The crack length and location along the beam height are characterized by a/l and h_2/h_0 ratios, in respect. Continuous material inhomogeneity in the height direction of the beam is characterized by S_{dh}/S_{gh} ratio. The continuous material inhomogeneity in the length direction at upper and lower surfaces of the beam is characterized by S_{gH}/S_{gh} and S_{dH}/S_{dh} ratios, respectively.

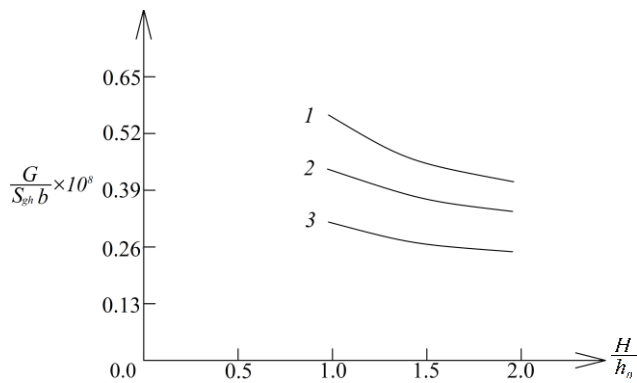


Figure 3. Strain energy release rate in non-dimensional form as a function of H/h_0 ratio (curve 1 at $h_2/h_0 = 0.2$, curve 2 at $h_2/h_0 = 0.5$ and curve 3 at $h_2/h_0 = 0.8$).

In order to evaluate the influences of varying beam height in longitudinal direction and crack location along beam height - on fracture behaviour, the strain energy release rate in non-dimensional form is presented as a function of H/h_0 ratio in Fig. 3 at three h_2/h_0 ratios for $S_{gH}/S_{gh} = 0.5$, $S_{dh}/S_{gh} = 0.6$, $S_{dH}/S_{dh} = 0.5$, $n = 0.6$, $r = 0.6$, $f = 0.6$, $m = 1.3$, $R = 0.1$ and $a/l = 0.7$. The curves in Fig. 3 indicate that the strain energy release rate decreases with increasing of H/h_0 ratio (this finding is attributed to the increase of beam stiffness). One can observe also in Fig. 3 that the strain energy release rate decreases with increasing of h_2/h_0 ratio (this behaviour is due to the increase of the stiffness of the upper crack arm).

The influence of material inhomogeneity in the beam height direction and crack length on the fracture behaviour is illustrated in Fig. 4, where the strain energy release rate in non-dimensional form is presented as a function S_{dh}/S_{gh} ratio at three a/l ratios. It can be observed in Fig. 4 that the strain energy release rate decreases with increasing of S_{dh}/S_{gh} ratio. The increase of a/l ratio leads to the increase of strain energy release rate.

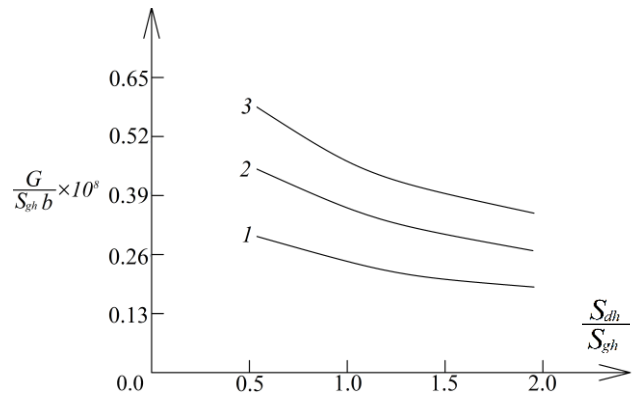


Figure 4. Strain energy release rate in non-dimensional form as a function of S_{dh}/S_{gh} ratio (curve 1 at $a/l = 0.3$, curve 2 at $a/l = 0.5$ and curve 3 at $a/l = 0.7$).

In order to evaluate the influence of continuous material inhomogeneity in the length direction at the upper and lower surfaces of the beam on the fracture behaviour, the strain energy release rate in non-dimensional form is presented as a function of S_{gH}/S_{gh} ratio in Fig. 5 at three S_{dH}/S_{dh} ratios. The curves in Fig. 5 show that the strain energy release rate decreases with increasing of S_{gH}/S_{gh} and S_{dH}/S_{dh} ratios, which is due from the increase in beam stiffness.

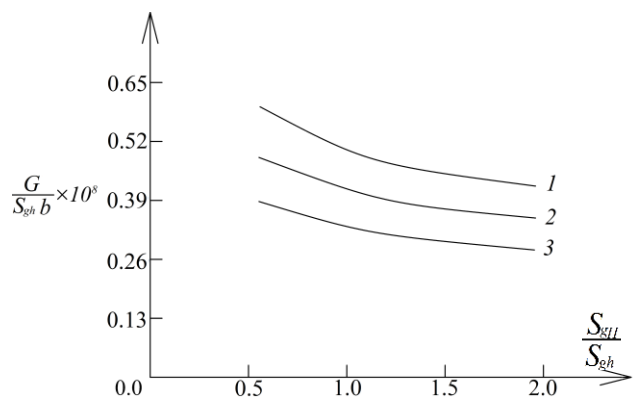


Figure 5. Strain energy release rate in non-dimensional form as a function of S_{gH}/S_{gh} ratio (curve 1 at $S_{gH}/S_{gh} = 0.5$, curve 2 at $S_{dH}/S_{dh} = 1.0$ and curve 3 at $S_{dH}/S_{dh} = 2.0$).

The influence of material property R , and width b , of the beam cross-section on the longitudinal fracture behaviour is also evaluated. For this purpose, calculations of strain energy release rate are carried out at various values of R . The results obtained are shown in Fig. 6, where the strain energy release rate in non-dimensional form is presented as a function of R at three values of b . One can observe in Fig. 6 that strain energy release rate decreases with increasing R . The analysis reveals that the increase in b leads also to the decrease of strain energy release rate (Fig. 6).

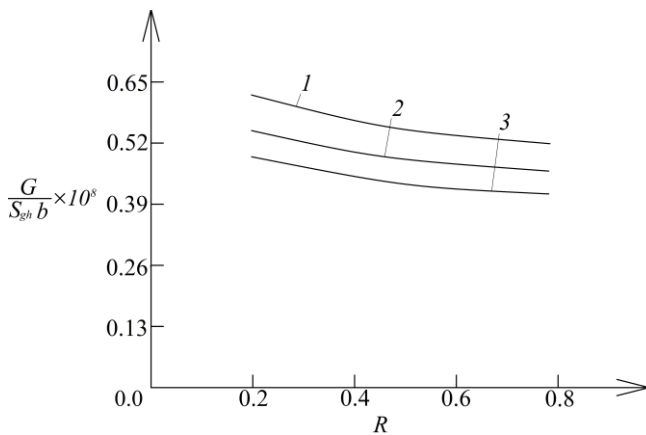


Figure 6. Strain energy release rate in non-dimensional form as a function of R (curve 1 at $b = 0.008$ m, curve 2 at $b = 0.009$ m and curve 3 at $b = 0.010$ m).

CONCLUSIONS

Longitudinal fracture behaviour of an inhomogeneous beam configuration with linearly varying height of the cross-section along beam length is analysed.

The beam is subjected to three-point bending. The cross-section of the beam is a rectangle. A longitudinal crack is located arbitrary along the beam height. Thus, cross-sections of the two crack arms have different heights. Besides, the height of the lower crack arm varies linearly in the length direction. The beam under consideration exhibits continuous material inhomogeneity in both height and length directions. The analysis is performed assuming nonlinear elastic mechanical behaviour of the material. The longitudinal fracture behaviour is studied in terms of strain energy release rate. For this purpose, a solution to the strain energy release rate is derived by considering the balance of energy. In order to verify the solution, longitudinal fracture is also analysed by applying the J-integral approach. The solution to the strain energy release rate is used to investigate the influences of various factors, such as the linearly varying height of the beam cross-section along the beam length, the crack location along beam height, the continuous material inhomogeneity along the height and length of the beam, the crack length and the width of the beam cross-section on longitudinal fracture behaviour. The investigation reveals that the strain energy release rate decreases with increasing of H/h_0 ratio. Concerning the influence of crack location along the beam height, it is found that the strain energy release rate decreases with increasing of h_2/h_0 ratio. It is found also that strain energy release rate increases with the increase of a/l . With respect to the influence of material inhomogeneity on fracture behaviour, the analysis shows that the strain energy release rate decreases with increasing of S_{dh}/S_{gh} , S_{gH}/S_{gh} , and S_{dH}/S_{dh} ratios. The analysis also reveals that strain energy release rate decreases with increasing of R and the beam width.

The analysis developed in the present paper can be used in preliminary structural design of inhomogeneous nonlinear elastic load-bearing beam structures of smoothly varying height of the cross-section along the beam length for evaluating the effects of longitudinal fracture.

REFERENCES

- Hirai, T., Chen, L. (1999), *Recent and prospective development of functionally graded materials in Japan*, Mater. Sci. Forum, 308-311(2): 509-514. doi: 10.4028/www.scientific.net/MSF.308-311.509
- Gasik, M. (2010), *Functionally graded materials: bulk processing techniques*, Int. J. Mater. Prod. Techn. 39(1-2):20-29. doi: 10.1504/IJMPT.2010.034257
- Yan, W., et al. (2016), *Multi-scale modelling of electron beam melting of functionally graded materials*. Acta Mater. 115: 403-412. doi: 10.1016/j.actamat.2016.06.022
- Saiyathibrahim, A., Subramaniyan, R., Dhanapal, P. (2016), *Centrifugally cast functionally graded materials - a review*. In: Int. Conf. on Systems, Science, Control, Communications, Engineering and Technology (ICSSCET 2016), Vol.02: 68-73.
- Erdogan, F. (1995), *Fracture mechanics of functionally graded materials*, Comp. Eng. 5(7): 753-770. doi: 10.1016/0961-9526(95)00029-M
- Tilbrook, M.T., Moon, R.J., Hoffman, M. (2005), *Crack propagation in graded composites*, Comp. Sci. Technol. 65(2): 201-220. doi: 10.1016/j.compscitech.2004.07.004
- Carpinteri, A., Paggi, M., Pugno, N. (2006), *An analytical approach for fracture and fatigue in functionally graded materials*, Int. J. Fract. 141(3-4): 535-547. doi: 10.1007/s10704-006-9012-y
- Rizov, V.I. (2017), *Analytical study of elastic-plastic longitudinal fracture in a functionally graded beam*, Strength, Fract. Complexity, 10(1): 11-22. doi: 10.3233/SFC-170197
- Rizov, V.I. (2018), *Delamination in multi-layered functionally graded beams – an analytical study by using the Ramberg-Osgood equation*, Struct. Integ. and Life, 18(1): 70-76.
- Rizov, V.I. (2018), *Delamination in nonlinear elastic multi-layered beams of triple graded materials*, Struct. Integ. and Life, 18(3): 163-170.
- Mahamood, R.M., Akinlabi, E.T., *Functionally Graded Materials*, Springer Int. Publ., 2017. doi: 10.1007/978-3-319-53756-6
- Lukash, P.A., *Fundamentals of Nonlinear Structural Mechanics*, Stroizdat, Moscow, 1978. (in Russian)
- Broek, D., *Elementary Engineering Fracture Mechanics*, Springer Netherlands, 1982. doi: 10.1007/978-94-009-4333-9

© 2020 The Author. Structural Integrity and Life. Published by DIVK (The Society for Structural Integrity and Life 'Prof. Dr Stojan Sedmak') (<http://divk.inovacionicentar.rs/ivk/home.html>). This is an open access article distributed under the terms and conditions of the Creative Commons Attribution-NonCommercial-NoDerivatives 4.0 International License